The design and performance of the wheel systems in the common foreoptics of the ELT METIS

Shiang-Yu Wang*[a], Richard C. Y. Chou[a], Masahiko Kimura[a], Hsin-Yo Chen[a], Pin-Jie Huang[a], Niels Tromp[b], Daan Zaalberg[b], Dennis Dolkens[b], Mirka Maresca[b], Ivan Lloro[b], Jeff Lynn[b], Jean-Christophe Barriere[c], Olivier Corpace[c], Olivier Absil[d], Gilles Orban de Xivry[d], Gert Raskin[e], Salman Muhammad[e]

[a] Institute of Astronomy and Astrophysics, Academia Sinica, Taipei, Taiwan; [b] NOVA optical infrared instrumentation group at ASTRON, Oude Hoogeveensedijk 4, 7991PD, Dwingeloo, The Netherlands; [c] Groupe LFEPS, Service d'Astrophysique, CE Saclay DSM/DAPNIA/Sap, 91191 Gif sur Yvette Cedex, France; [d] Department of Astrophysics, Geophysics & Oceanography, Université de Liège, 17 allée du Six Août, bat B5c, 4000 Liège, Belgium; [e]Institute of Astronomy, K.U.Leuven, Celestijnenlaan 200D, B-3001, Leuven, Belgium

ABSTRACT

The Mid-infrared ELT Imager and Spectrograph (METIS) is one of the first light instruments for the Extremely Large Telescope (ELT) and will cover the thermal- and mid-infrared (3–13 μm). With the single conjugate adaptive optics (SCAO) system, it will enable high contrast imaging and integral field unit (IFU) spectroscopy (R ~ 100 000) at the diffraction limit of the ELT. Inside the METIS cryostat, it has a modular design and is composed of the common fore optics (CFO), the imager (IMG), the SCAO, and the L and M band integral field spectrograph (LMS). The components are cooled down to around 60K, or lower for the detectors, during the operation to reduce the background. In the CFO of METIS, four wheels are inserted in the optical path including the atmospheric dispersion corrector (ADC) wheel, the pupil plane one (PP1) wheel, the focal plane two (FP2) wheel and the LMS pickoff wheel. The PP1 wheel and the ADC wheel are located near the first pupil plane while the other two wheels are at the second focal plane. These wheels accommodate the optics, slits, masks and filters for various operation modes of METIS. In each wheel, common cartridges are designed to hold the optical elements to facilitate an easy exchange between them. High positioning repeatability is required for some of the optics. We will report the design and the initial integration and tests of the wheels in this paper.

Keywords: Cryogenic, mid-infrared, wheels, mechanism, ELTs

1. INTRODUCTION

The METIS is one of four first-generation instruments on ESO's ELT. With its coverage of the thermal- and mid-infrared wavelength range (3 – 13 μm), METIS provides a unique and scientifically important observational capability, not only at the ELT but among the first generation of instruments on the 30-meter class telescopes in general. A general and brief overview of METIS can be found in the ESO Messenger[1]. METIS has two basic observational functionalities: 1) direct imaging at 3 – 13 μm, including medium resolution long-slit spectroscopy (R ~ 1400 at L/M band; R ~ 400 at N band) plus coronagraphy for high contrast imaging. 2) High resolution (R ~ 100,000) integral-field spectroscopy at 3 – 5 μm plus coronagraphy for high contrast IFU spectroscopy. The FoV of METIS is approximately 11 × 11 arcsec and the FoV for the IFU mode is 0.5 square arcsec. The high contrast imaging mode and the IFU are achieved with the aid of the SCAO[2].

Inside the METIS cryostat, it adopts a modular design. There are four major components: 1) the CFO which is the core structure of METIS that all subsystems are connected to. 2) the IMG[3] for the direct imaging as well as medium resolution spectroscopic observations. 3) the SCAO which provides diffraction limited observations; and 4) the LMS that provides high resolution integral field spectroscopic observations. The components are cooled down to around 60K, or

*sywang@asiaa.sinica.edu.tw; phone 886 2 2366-5338; fax 886 2 2367-7849; www.asiaa.sinica.edu.tw

Ground-based and Airborne Instrumentation for Astronomy X, edited by Julia J. Bryant, Kentaro Motohara, Joël R. D. Vernet, Proc. of SPIE Vol. 13096, 1309654
 · 0277-786X · doi: 10.1117/12.3018466

lower for the detectors, during the operation to reduce the background noise. Outside the METIS cryostat, a Warm Calibration Unit (WCU)[4] provides the necessary calibration source for METIS. The simplified optical layout of METIS is presented in Figure 1[5].

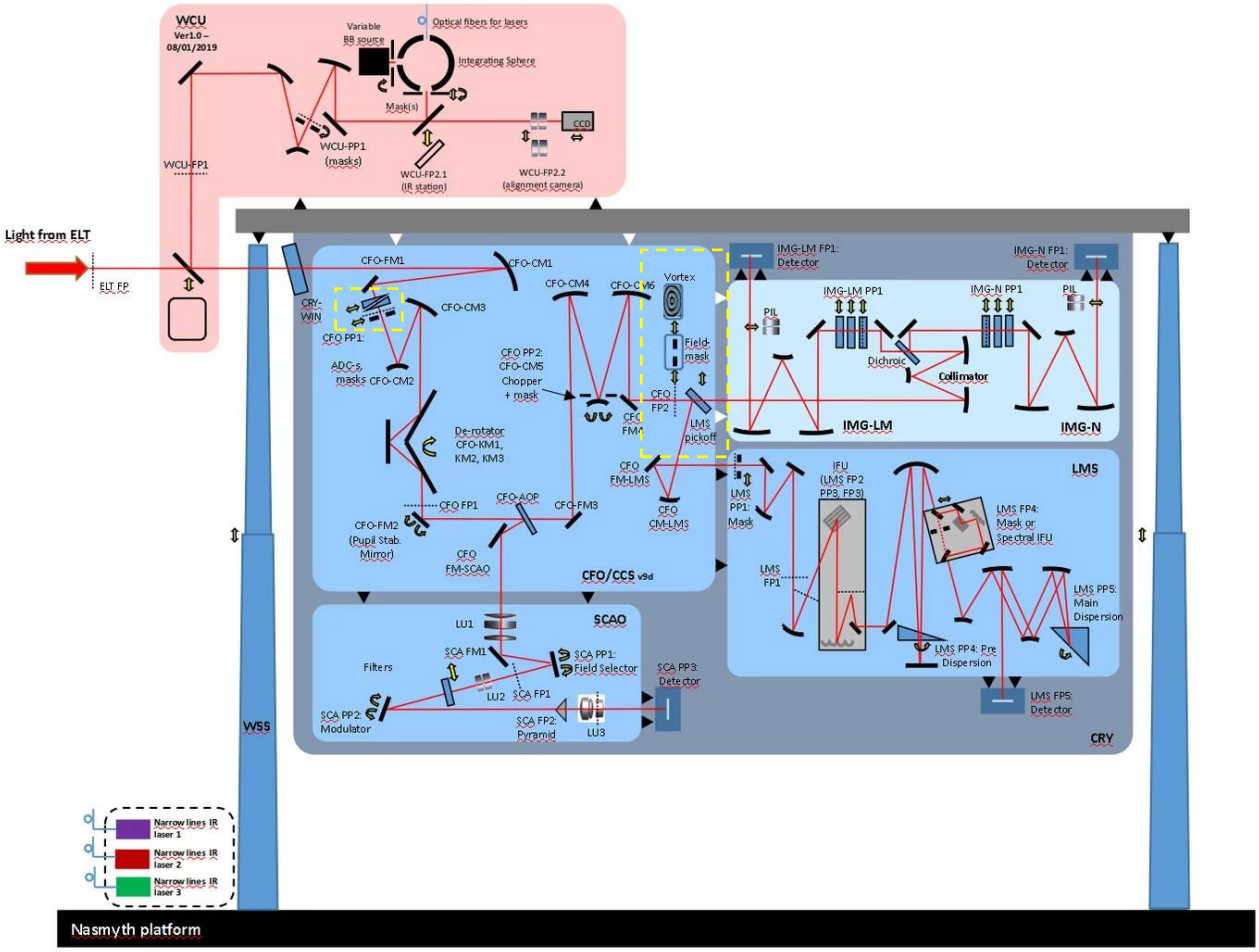

Figure 1. The schematics of METIS optical system with major components to show various operational modes of the instrument. Yellow boxes denote the locations of the wheels covered by this manuscript.

In the CFO of METIS, four wheels are inserted in the optical path. The PP1 wheel assembly includes the PP1 wheel and the ADC wheel. The FP2 wheel assembly consists of the FP2 wheel and the LMS pickoff wheel. The PP1 wheel assembly is located near the first pupil plane while the FP2 wheel assembly is at the second focal plane. The ADC wheel accommodates different prisms for the compensation of the atmospheric dispersion. The aperture masks and the vortex phased masks (VPMs) in the PP1 and FP2 wheels support various high contrast imaging modes for the IMG and LMS. The FP2 wheel also accommodates the slits for the LMS, field apertures and the Lyot Occulting Masks (LOM). The switching between the imaging and spectrographic mode is controlled by a mirror, a beamsplitter and an aperture on the LMS pickoff wheel. All wheels are actuated with the cryogenic motors called Indexed Cryogenic Actuator for Rotation (ICAR) developed by the CEA[6]. The yellow boxes in Figure 1 denote the locations of these wheels.

The METIS project had the major system final design review in late 2022 and ESO officially announced the METIS moves into the Manufacturing, Assembling, Integration and Verification (MAIV) phase in May 2024. Currently the FP2 wheel has passed the manufacturing readiness review and most of the parts have been fabricated. The manufacturing of the LMS pickoff wheel will start soon. The final adjustments of the design on PP1 and ADC wheels is on-going. In this

paper, we report the wheel design details in section 2 and 3, the prototyping and initial integration/tests results of the wheels in section 4 and a summary.

2. THE FP2 WHEEL ASSEMBLY

The FP2 wheel assembly contains the FP2 wheel and the LMS pickoff wheel. The wheels accommodate the final optical elements in the CFO optical path and are mounted with the wheel plane parallel to the gravity direction. The assembly consists of masks, slits, alignment/verification components, the beam splitter and the pickoff mirrors for the IMG, and the LMS. The two wheels have the same rotational axis but with separate mounting structures to the CFO. Both wheels were driven by the standard METIS ICARs and each ICAR is mounted on a spider vane structure which connects to the CFO. The two ICARs are not directly connected to each other to avoid unnecessary vibration couplings. If we follow the optical path, the whole assembly consists of the spider vane for FP2 wheel, the FP2 ICAR, the FP2 wheel, the spider vane for the LMS pickoff wheel, the LMS pickoff wheel ICAR and the LMS pickoff wheel. Figure 2 shows the FP2 assembly from two opposite directions of view and its position in the CFO.

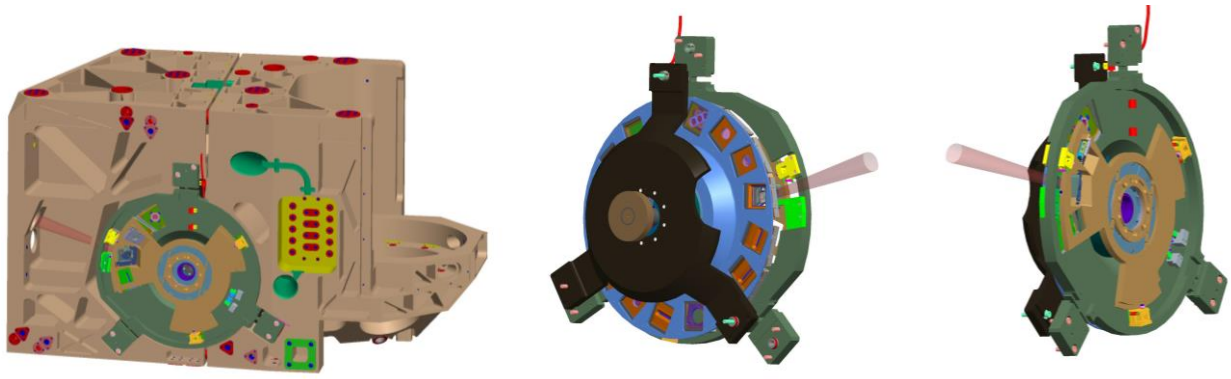

Figure 2. The FP2 wheel assembly mounted on the backbone structure of the METIS CFO (left), the front side of the assembly (middle) and the rear side (right) of the assembly.

2.1 The FP2 wheel

The overview of the FP2 wheel is shown in Figure 3. The top of the FP2 wheel locates two copper blocks that serve as counterweights. The counterweight and the ICAR are mounted on the opposite sides of the spider vane. The FP2 wheel body is connected on the rotor side of the ICAR. The total weight for the FP2 wheels is 26.9 kg and the center of gravity is at (0, 0, 70) mm with respect to the center of the ICAR interface. The counterweight helps to meet the load requirement of the ICAR and the space envelope requirements. The choice of a two-piece copper as counterweight was meant to reduce the diameter of the counterweight such that the whole assembly can fit inside the allowed envelope.

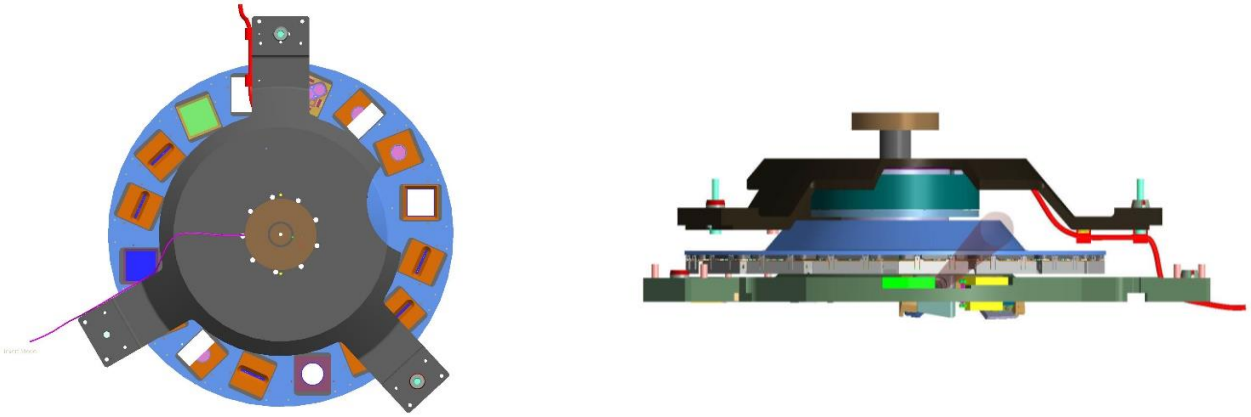

Figure 3. The top view (left) and side view (right) of the FP2 wheel structure.

The FP2 wheel accommodates 16 optical elements. These optical elements are mounted on cartridges which have the same dimensions to provide flexibility in replacing or swapping the optical elements without removing the wheel structure. It is important to keep the alignment as much as possible. Each cartridge is mounted on an intermediate plate which aims to facilitate the alignment process between the optical element and the incident optical beam. The required alignment accuracy varies from element to element. The elements with the tightest alignment tolerances are the VPMs, which need to be positioned with an accuracy of 25 milli-arcsec on sky or 83 μm on the FP2 wheel relative to the optical axis repeatedly. Since the tolerance chain is long between the optical elements and the FP2 wheel interface to the CFO, the intermediate plate provides the adjustment mechanism which simplifies the alignment process and relaxes the manufacturing tolerance of FP2 wheel and cartridges. Figure 4 shows the intermediate plate and the relationship between the cartridge elements and the intermediate plate. Three contact pads to the cartridge bed and two holes for the dwell pins are designed on the intermediate plate to keep good positioning accuracy.

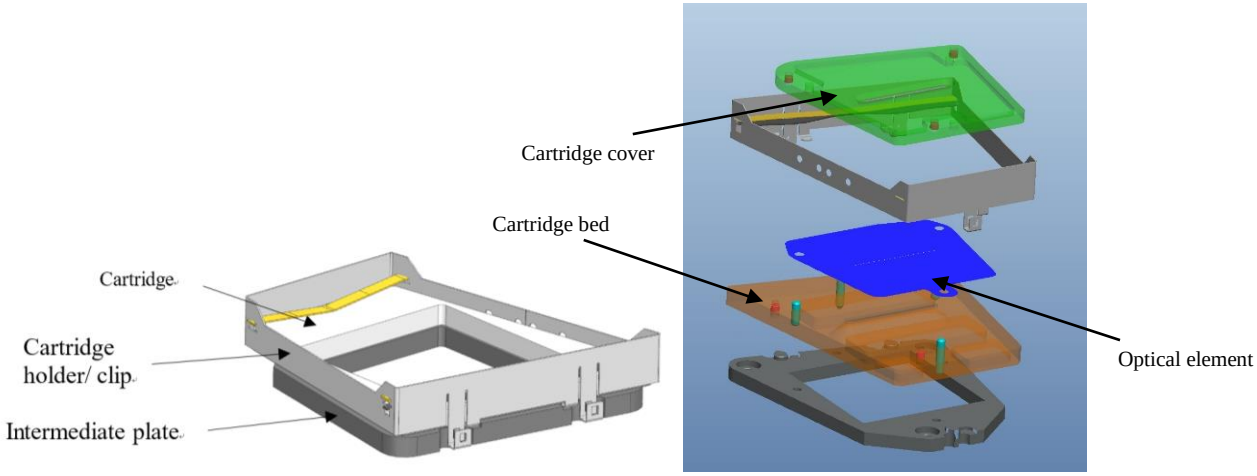

Figure 4. The intermediate plate components (left) and the relationship with cartridge components (right).

These intermediate plates and cartridges will be accurately positioned on the wheel first using the Intermediate Plate Alignment Tool (IPAT), a mechanical reference that ensures consistent accurate positioning of all FP2 elements to the same reference. The IPAT will be temporarily mounted on the still available accurately repeating mounting points, normally used for the LMS pickoff wheel. To ensure that the FP2 target will be aligned with the established optical axis, a reference intermediate plate will be used. Both IPAT and the reference intermediate plate are shown in Figure 5. By observing features on this reference intermediate plate with the alignment telescope, the initial misalignment of the reference intermediate plate relative to the IMG alignment and verification tool is measured. A shim part inside the tool is subsequently milled to correct for any lateral misalignment and from then the tool is calibrated and permanent. The IPAT provide a precision stage so that the cartridges can be inserted on the FP2 wheel accurately and smoothly.

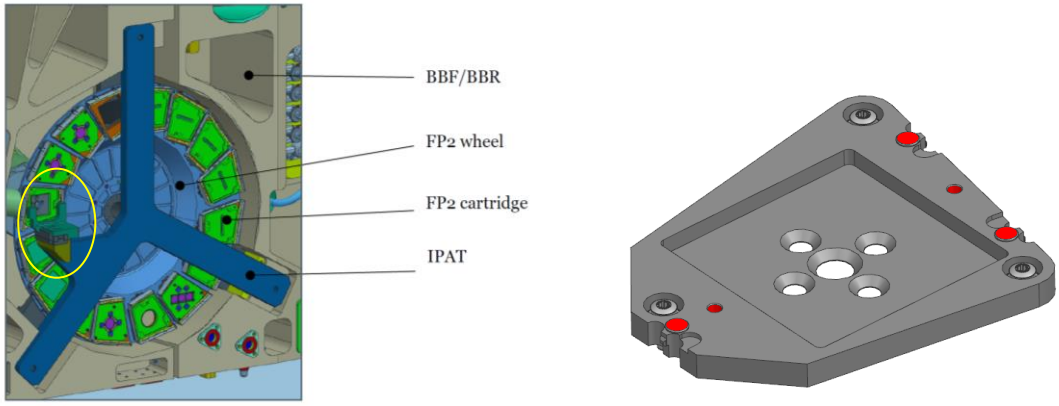

Figure 5. The IPAT (left) and the reference intermediate plate (right). The yellow circle denotes the accurate mounting stage.

The FP2 cartridges can be divided into three types (slit/field mask, LOM and VPM) depending on how the optical element is mounted. The 16 optical elements are listed in Table 1.

Table 1. The list of the optical element installed on the FP2 wheel.

Number	Name	Description
01	FIELD-11	Field-Mask 11"x11" square
02	PI-MASK	30 mm circular mask to be used with pupil imaging mode in IMG-LM and IMG-N.
03	VPM-L	VPM for L band
04	VPM-M	VPM for M band
05	FIELD-3	Field-Mask 3" circular
06	FIELD-14	Field-Mask 14"x14" square
07	LOM-LM	LOM for LM bands
08	LOM-N	LOM for N band
09	PNH-1	Calibration and AIV pinholes.
10	SLIT-A	19.0 mas slit
11	SLIT-B	28.6 mas slit
12	SLIT-C	38.1 mas slit
13	SLIT-D	57.1 mas slit
14	SLIT-E	114.2 mas slit
15	ALIGN + DARK	Alignment mask for AIV. It can also be a dark.
16	VPM-N (x3)	VPM for N band

Each type of cartridge has different mechanical mounts based on the size and material of the optical elements. The field apertures and slit masks are made of 50 μm thick SUS304 foil. The LOMs are made of 5 mm ZnSe substrates with 20mm diameter, and the VPMs are fabricated with 300 μm thin diamond substrates with 20 mm and 15 mm diameters. The cartridge mounts are designed to hold the optical elements within the tolerance in both radial and axial directions and also accommodate the possible CTE difference during the warming and cooling process without shifting or damaging the optics. Figure 6 shows the layout of the three types of cartridges and their corresponding explosive diagrams. The typical dimension tolerance of the cartridge components is around ±10 μm.

The mask type cartridge is the simplest cartridge to mount the SUS304 mask foil. Three positioning pins on the bed plate are used for the alignment between the mask and the cartridge. To absorb the CTE differences between the aluminum bed and the SUS304 mask, three radially elongated grooves are added on the mask plate while the width matches the pin size. The accuracy of the pins and the grooves is around 8 μm. An aluminum cover plate (green plate in Figure 6) is designed to cover the mask. Three magnets (red cylindrical dots) are used to provide the clamping force to hold the mask at the correct axial position. The top cover is held by the three pins with the cartridge bed. The whole cartridge will be installed on the intermediate frame guided by 2 positioning pins so that the alignment accuracy can be secured.

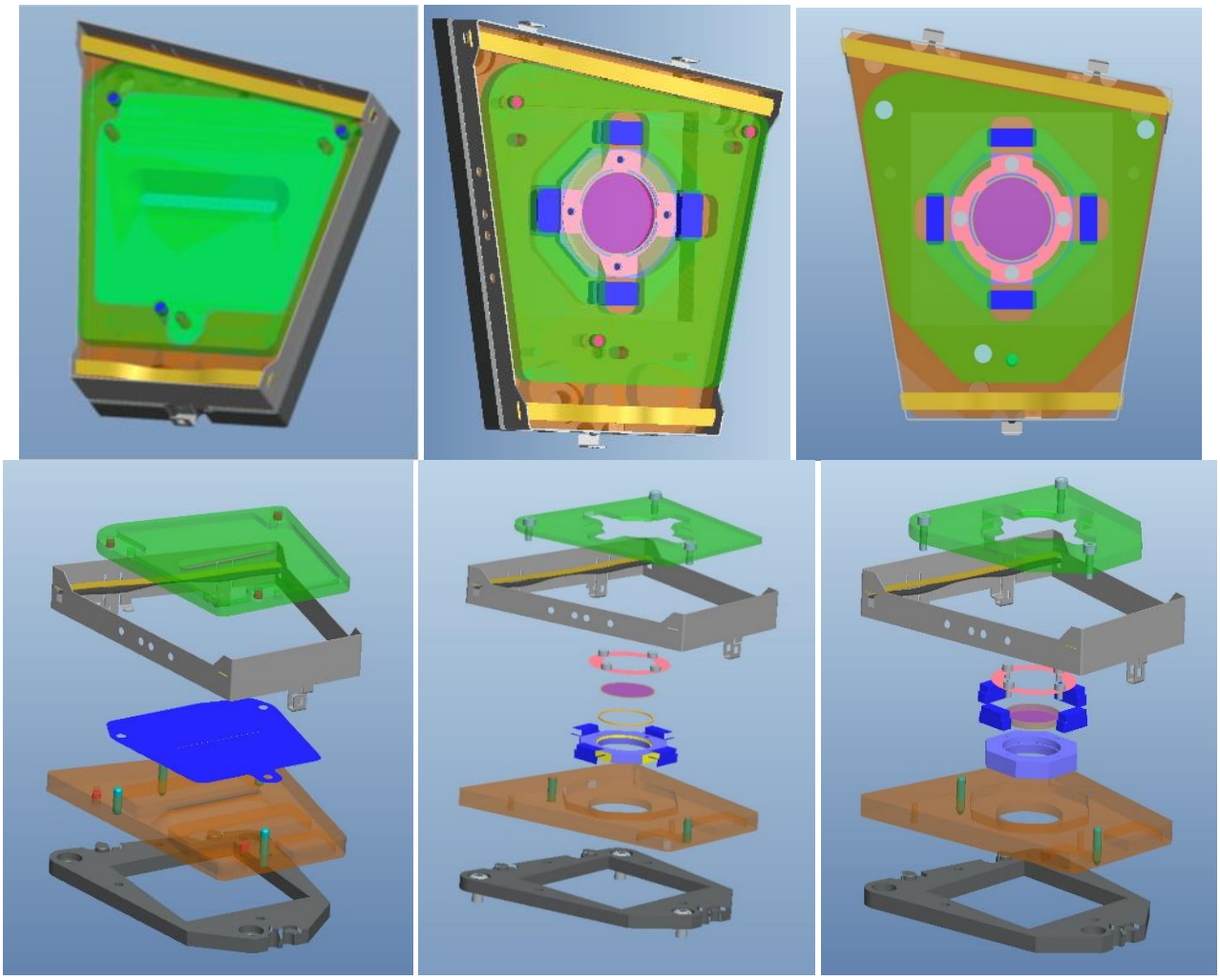

Figure 6. The top row shows the overall layout of the three different types of FP2 cartridges and the bottom row shows the corresponding explosive diagram of the cartridges. From left to right shows the mask type, VPM type and LOM type cartridges, respectively.

The mechanical design for the VPM and the LOM cartridges is similar. A chromium frame is used as the optics holder because chromium has the closest CTE to diamond and ZnSe while it is free from the rust issue. Four polyoxymethylene (POM) blocks surrounding the chromium frame serve as buffers to absorb the CTE differences. The thickness of the POM blocks has been calculated (ranging 6 – 8 mm) so that it can fully compensate for the CTE differences btween aluminum and chromium. To achieve the required positioning accuracy, SUS304 shims will be inserted between the chromium frame and the POM blocks to adjust the position of the VPMs. Since the diamond plates are thin, the design uses ductile washers to spread the pressure evenly around the VPM. A thin platinum washer is added between the diamond substrate and the chromium frame. On top of the optics, a gold plated SUS304 retaining ring with thickness of 50μm is used to provide the clamping force. The analysis shows the clamping force exerted is less than 1.5N as required. The final alignment of the VPMs with the cartridges will be carried out with an IR camera in the University of Liège. After the alignment is completed, specific shims with correct size will be manufactured and inserted in the cartridge to secure the alignment. For the LOM optics, it is critical that the mount does not generate too much stress on the optics. To avoid the birefringence issue, the clamping force exerted is less than 1 MPa for the LOM optics. Similar to the mask type cartridges, a top cover is used to hold the chromium frame and the bed plate has the same interface to the intermediate plate.

It should be noted that the VPM-N cartridge has to accommodate three masks. As the alignment requirement for the VPM-N only applies to the central mask, we designed a chromium frame to hold the three masks. The design also includes four POM blocks and shims for alignment. Due to the space limitation, the four POM blocks are not facing each other but this should not affect the alignment accuracy.

To populate the cartridges on the FP2 wheel, it is arranged so that the center of mass is close to the center of the wheel while keeping the same type of cartridges together as much as possible. The offset of CG is 0.090 mm and 0.086 mm away from the ICAR geometrical center in x and y directions, respectively. Figure 7 shows the configuration of the FP2 wheel, the order of the cartridge follows the order shown in Table 1.

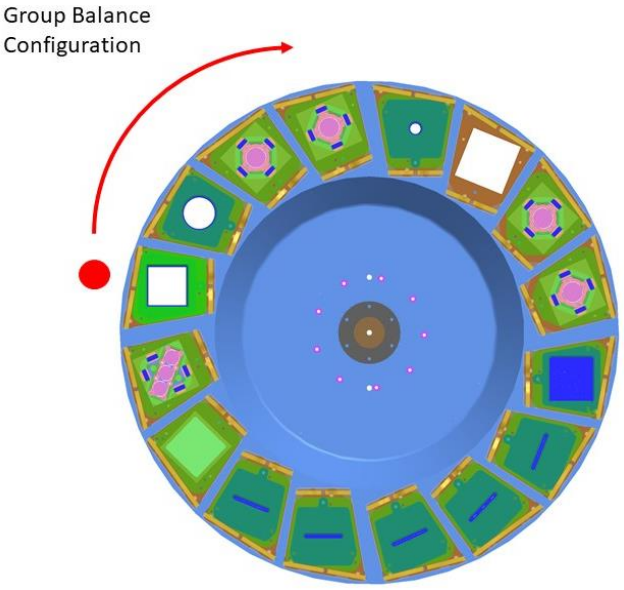

Figure 7. The cartridge distribution of the FP2 wheel. The order of the cartridge follows the order shown in Table 1 and the red dot denote the first cartridge.

2.2 The LMS pick-off wheel

The LMS pick-off wheel locates at the end of the optical path inside CFO, it delivers light either to IMG or LMS or both depending on different operation modes. The LMS pickoff wheel contains three elements: the LMS pickoff mirror, the beam splitter and an open slot. A beam splitter is located on the LMS pickoff wheel such that the components on the FP2 wheel can be used with both IMG and LMS.

The optical path through the pickoff wheel to the LMS via the pick-off mirror is relatively long, so that the requirements to the pickoff mirror repeatability are quite stringent. The repeatability requirement of the LMS pickoff mirror is less than ± 10 μm for shift in the radial (Y) and axial (Z) directions and less than ± 10 arcsec in tilt. Unfortunately, the ICAR specifications could not meet the requirements as the wobbling and the repeatability of the ICAR is larger than the required numbers. The radial runout of ICAR rotor interface is ± 40 μm and radial run-out repeatability is ± 10 μm. These ICAR repeatability errors yields non-compliant LMS pickoff mirror tilt and shift even without considering the possible errors of the wheel itself. Hence, the LMS pick-off wheel adopts special designs to mitigate the variation generated from the ICAR, including 1) four special hinges locate at the wheel center to absorb the ICAR wobbling, 2) spring loaded bearings mounted on a retaining structure to guide the wheel movement, 3) thin necks for the three interface pads to isolate the pickoff wheel system from the CFO interface repeatability. The LMS pickoff wheel layout is shown in Figure 8. The design has gone through various analysis and tradeoffs. The orientation and thickness of the hinges, the bearing mounting structure and the interface neck width have all been optimized so that the structure is weak enough to provide the flexibility to absorb the possible ICAR shifts which it is stiff enough so that the structure will not deform due to the weight of the structure when the wheel rotates.

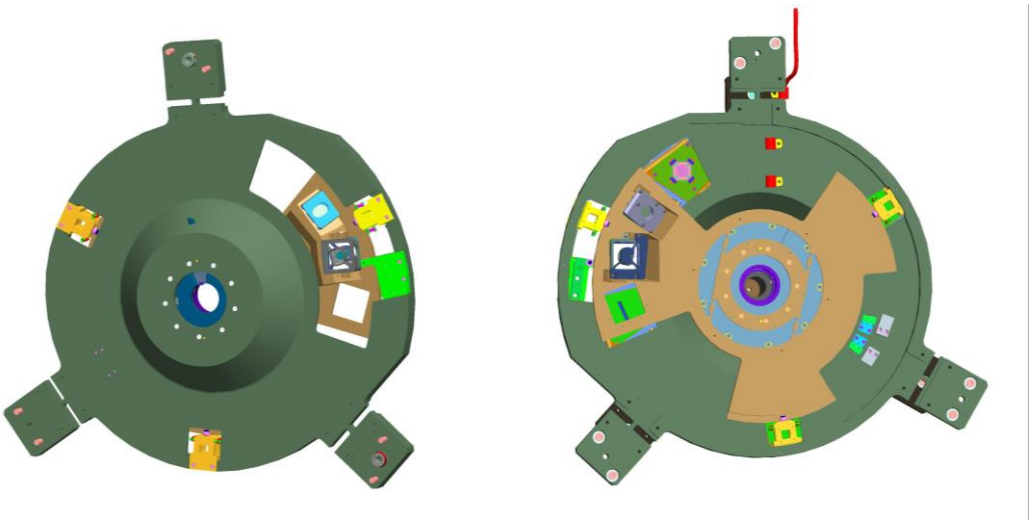

Figure 8. The front side (left) and the rear side (right) of the LMS pickoff wheel.

A closer view of the hinge and the bearing mounting structure are shown in Figure 8. The hinges are oriented to absorb the ICAR wobbling in the radial direction while considering the force coming from the clamping bearings of the fans. Cryogenic bearings were mounted on the supporting structure to clamp the wheel in the radial and axial directions. The axial bearings are added on the three fans of the pickoff wheel to avoid the possible tilt of the wheel. Since the optics are all on one fan, a radial spring loaded bearing is added on this particular fan. The bearings used are the same as the ones from GRW for the MATISSE instrument of the VLT. From the experience of MASTISSE, the lifetime of the bearings depends on the pre-loading force. It is important to keep a low loading force, so we set the target load to be ~20N. Each spring loaded bearing assembly contains two bearings and is made of a single aluminum block to minimize the possible manufacturing error and also ensure good orientation control of the bearing. The design keeps the bearings to be tangential to the rotation direction of the wheel. Two stainless springs are located at the sides of the block to provide the clamping force of 20 N in the axial direction while the mounting structure is weak enough not to exert additional force on the bearings generated from the manufacturing errors. The design avoids the difficulties to control the preloading force purely from the mounting structure. The radial bearing assembly also provides the clamping force of 20 N in the radial direction. A SUS304 spring is used to push a bearing mounted block towards the wheel body to provides the clamping force in the radial direction. The bearing contacting surface of the pickoff wheel will be PTFE (Nituff) coated to enhance the durability during the METIS operation. To verify the bearing guide and the hinge concept, a prototype of the LMS pickoff wheel was produced and tested to demonstrate the wheel repeatability satisfies the requirements. More details are described in section 4.

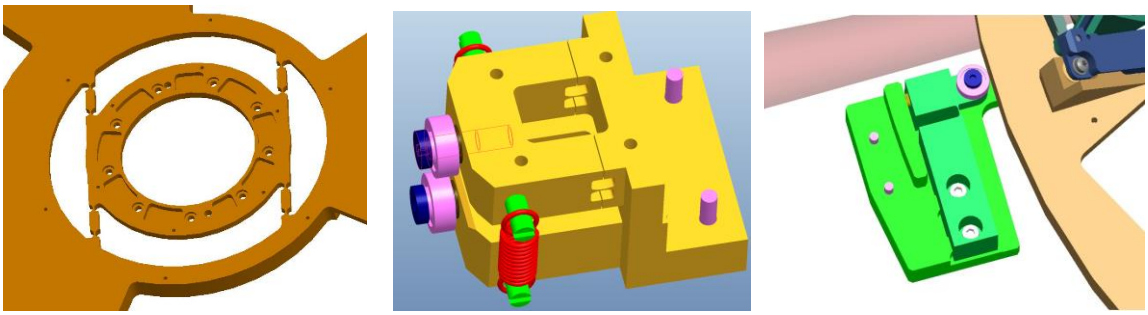

Figure 9. The hinge structure (left), the axial bearing mounting structure (middle) of the radial bearing mount for the LMS pickoff wheel.

3. THE PP1 WHEEL ASSEMBLY

The ADC wheel and the PP1 wheel share the same mounting frame to the CFO. Both ADC and PP1 wheels are driven by a standard METIS ICAR and both ICARs are also mounted on the mounting frame. The allowed space for the PP1 wheel assembly in CFO is tight due to its location inside the cryostat. The design principle has been focused to make it compact. Figure 9 shows the mechanical layout of the PP1 wheel assembly. Most of the PP1 wheel assembly is inside the CFO structure so it is well protected and covered. The extended part of the wheel assembly outside of the CFO allows an easy access to individual optical elements on the wheel. Both ADC-1 and ADC-2 shall be used in parallel with some of the PP1 elements. As a result, the distance between the ADC wheel element and the PP1 wheel element has to be smaller than 20 mm. In order to meet the requirement, the two wheels are facing each other closely. In addition, an aluminum plate is added between the two wheels to enhance the thermal radiation to cool down or warm up the wheels. This makes the allowed space very tight. The cartridges of the wheels are mounted from opposite sides of the two wheels.

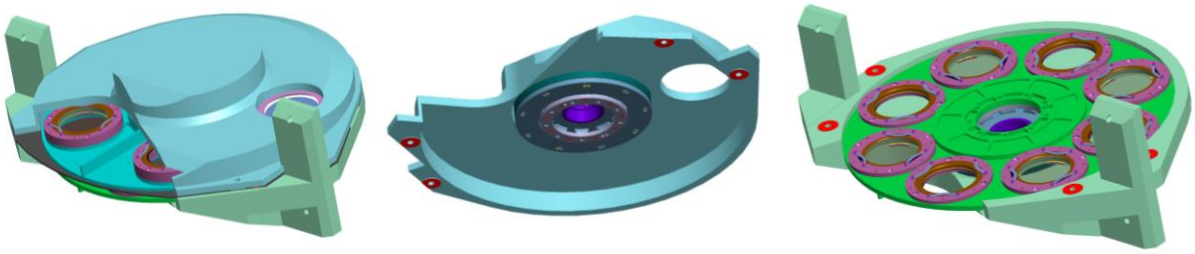

Figure 10. The PP1 wheel assembly (left), the top structure that mount the ICAR for the ADC wheel (middle) and the PP1 wheel on the bottom structure (right).

3.1 The ADC wheel

The ADC wheel has five slots for the cartridges. Two positions are reserved for two sets of the ADC prisms. The other positions accommodate two circular open masks and one circular ZnSe optics for AIV purposes. Although a common cartridge design is preferred to allow interchangeable cartridges, the cartridges have two sizes on the ADC wheel. The ADC cartridges are slightly larger than the other elements because the ADC prism size is larger. Given that the chance for exchanging the ADC and other filter elements is low, this provides a merit of reducing wheel weight by adopting a slightly smaller cartridge design for non-ADC elements. The potential alignment accuracy of the mask is affected by two main factors. One is the ICAR rotational uncertainties; the other one is the manufacturing errors of the cartridge itself. For ICAR rotational uncertainties, the translational error is ± 50μm (including ICAR offset of center rotation and radial wobbling). For cartridge manufacturing errors, the position accuracy is roughly ± 50μm. The current design can satisfy the requirement of the ± 100μm alignment accuracy of the optical elements in rotation for the pupil plane. Figure 11 shows the mechanical layout and the explosion diagram of the cartridge designs in the ADC wheel.

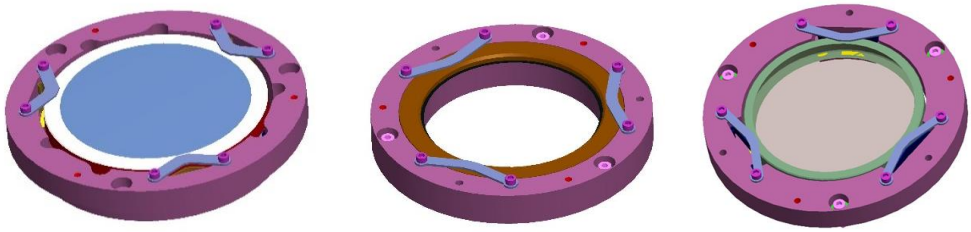

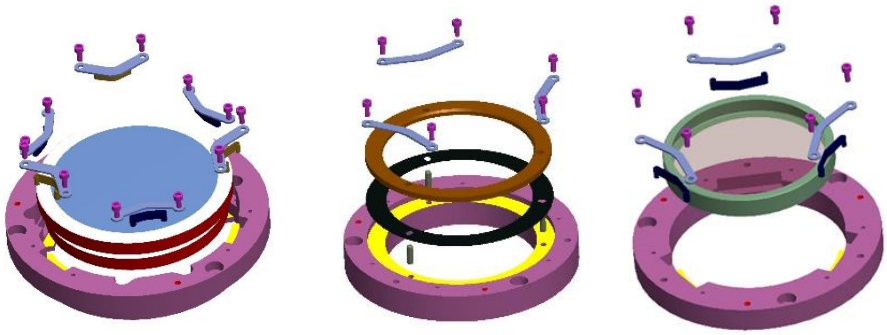

Figure 11. The top row shows the overall layout of the three different types of ADC wheel cartridges and the bottom row shows the corresponding explosive diagram of the cartridges. From left to right shows the ADC cartridges, mask type cartridges and the ZnSe type cartridges, respectively.

The ADC prisms are mounted inside an aluminum frame. The reference plane (yellow parts in Figure 11) inside the aluminum frame provides the reference position between the ADC prisms. Six springs made of SUS304 are used to secure the position accuracy of the prisms while absorbing the CTE differences among different materials. Three blue springs are dedicated for the bottom prism and the brown springs are for the top prism. On top of the prisms there are also three SUS304 leaf springs that provide the necessary clamping force. Screws and pins are used to fix the aluminum frame to the wheel body.

The middle column in Figure 11 shows the mechanical layout of the mask type cartridge. The design is similar to the FP2 mask cartridges. The circular masks made of SUS304 with thickness of 50μm will be mounted on the cartridge via three positioning pins. To absorb the CTE differences between the aluminum frame and the steel mask, three radially elongated grooves are engraved on the mask foil. An aluminum cover plate is designed to cover the mask. Three SUS304 leaf springs are used to provide the necessary axial clamping force. The mechanical design for the ZnSe cartridges adopts similar concept as the ADC cartridge. An aluminum frame is used to hold the optics, and three SUS304 springs between the aluminum frame and the optics are used to maintain the optics centering accuracy while absorbing the CTE differences. Three leaf springs with a thickness of 50μm located on top of the aluminum frame are used to provide the axial clamping force for the optics. Screws are used to fix the aluminum frame to the wheel body

3.2 The PP1 wheel

The PP1 wheel is located 5 mm below the ADC wheel. There are eight elements on the wheel: four open circular apertures, three ZnSe circular optics and one Zerodur element. The elements on the PP1 wheel also adopt the cartridge design used for the ADC wheel. All cartridges on the PP1 wheel have the same dimensions. The cartridge design basically follows the mask type and ZnSe type design as in the ADC wheel. Compared with the ADC cartridges, the main difference lies in the thickness of the top retaining ring because the PP1 cartridges are installed in the opposite direction to those of the ADC. A different retaining ring thickness is used to adjust the position of the masks/optics to fit the location of the pupil plane. For the Zerodur cartridge, the design is the same as the ZnSe one, the main difference lies in the thickness and shape of stainless springs which compensate the CTE differences between the materials.

4. PROTOTYPING AND MANUFACTURING OF WHEELS

Currently, the FP2 wheels are in the manufacturing phase and the manufacturing of the LMS pickoff wheel will start soon. The final design and drawings of the PP1 wheels are still in progress. In this section we report the repeatability tests of the prototype LMS pickoff wheel and the initial inspection of the FP2 wheel components.

4.1 The prototype of LMS pick-off wheel

Since the design of the LMS pickoff wheel is unique and critical to the performance of METIS, we conducted a prototype to check the repeatability for the LMS pick-off wheel to verify the concepts of the hinge structure introduced to alleviate the ICAR rotation uncertainty in early 2022. The prototype is shown in Figure 12. Compared with the current LMS pickoff wheel design, the prototype structure has the same structure of the hinges but the number of bearings and the mounting structure are different. In the prototype design, there are two leaf spring assemblies locate on the fan that resides the optical elements of the wheel. The clamping force of the bearings is around 80N. The corresponding retaining ring is only 1/3 of a full circle. Also, it does not have the thin neck for the interface structure. All the design change to the current design were based on what we learned from the prototype tests.

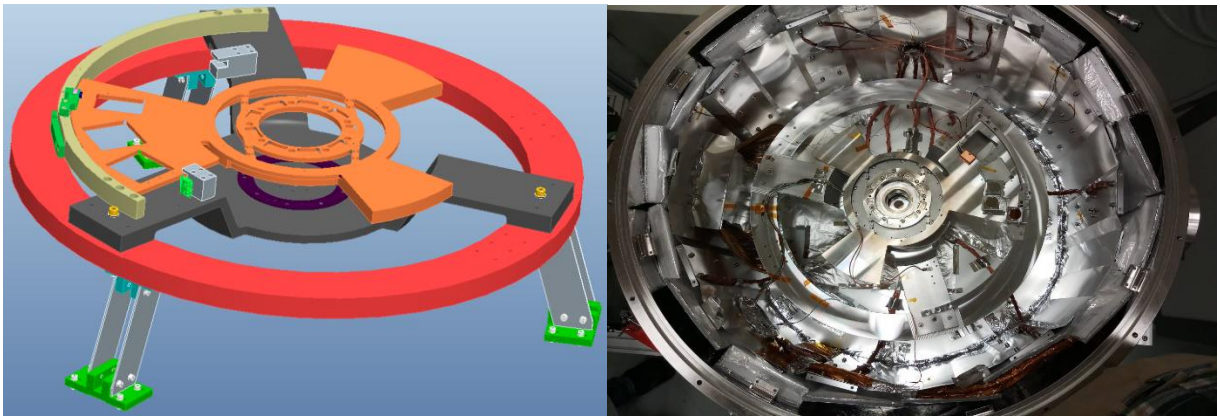

Figure 12. The layout of the prototype LMS pickoff wheel (left) and a picture of the wheel inside the test cryostat (right).

The entire prototype wheel sat on an aluminum ring and the ring was supported by three G10 legs for thermal isolation. The cryostat has two separate chambers. The large one contains the pick-off wheel and a smaller one attached to the larger one through a neck and the main cooler CRYOMECH PT60 was mounted directly to the small chamber. It allows us to install the wheel at horizontal position and rotate the big chamber afterwards to vertical direction for the measurement. To detect the shift of the wheel in the axial and radial directions, a laser was shot through the cryostat window to a folding mirror installed on the wheel body and a small CMOS camera was used outside the cryostat to capture the reflected laser spot. Another laser was also mounted on the same structure but shot directly to the CMOS camera without going through the pick-off wheel as a reference to remove the vibration and drift of the setup. Note that this method cannot differentiate the direction of the wheel shift. What we presented here are the measured value and the worst cases assuming the drifting is solely in one direction as an upper limit. The tilt of the prototype wheel was measured by a Triopics autocollimator. Figure 13 shows the overall test setup.

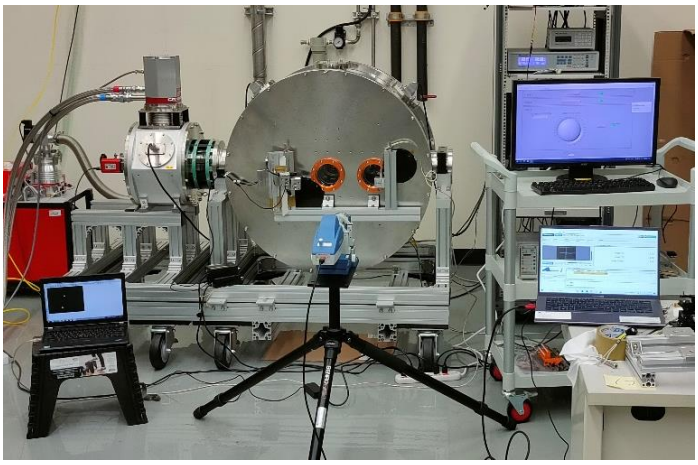

Figure 13. The testing setup of the prototype LMS pickoff wheel.

The cooling down and warming up processes roughly takes one week each. The repeatability test was conducted around 70K. Each test was conducted by moving the pick-off wheel between the two optics slots for 18 times. The derived wheel body shifts and tilts were recorded. Figure 14 shows the results. The left panel shows the measured shift and the right panel shows the measured wheel body tilt by the autocollimator. In most cases, the measured shift and tilt meet the required ± 10 μm and ± 10 arcsec value. Although the derived upper limit in y direction (radial direction) exceeds the requirements at #15 and 16 rotations, in reality, the probability that the shift of the wheel to be solely in one direction and exceeds the +/-10 μm requirement is low. We have repeated the same tests for several times on different day and consistent results were obtained. On the other hand, we also tried to run the system for ~ 500 cycles to see the possible wear of the mechanical structure. We found some dusts on the wheel body after the tests. This leads to the modification of the design with PTFE (Nituff) coating and well controlled preloading force of the bearings.

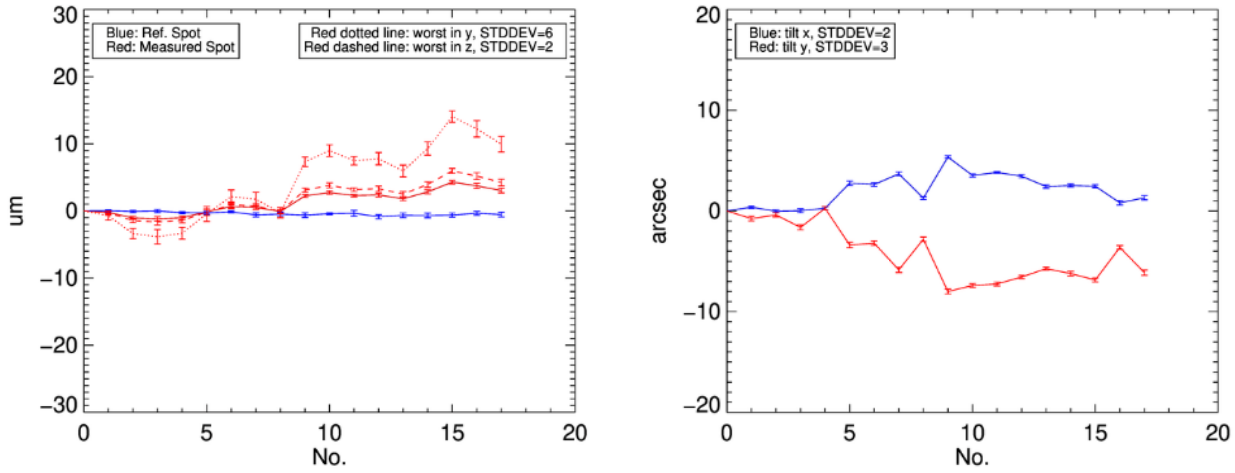

Figure 14. The shift of the prototype LMS pickoff wheel for 18 continuous wheel movements (left). The blue curve indicates the shift of the reference spot while the red solid curve shows the mixed shift in radial and axial directions. The red dotted and dashed lines represent the worst case when all the measured values were attributed to one axis, thus the upper limits. The right panel shows the tilt of the wheel measured by the autocollimator.

4.2 The manufacturing of FP2 wheel

The FP2 wheel passed the manufacturing readiness review in Sep. 2023. All the FP2 wheel parts have been manufactured. The aluminum alloy AL6061 T651 is used for the majority of the wheel components. To maintain the long-term stability of the parts with thermal cycles during the operations, smaller raw blocks had gone through deep cooling treatment before the manufacturing process started and the material for large pieces such as wheel body and the spider supporting structure had gone through not only the deep cooling treatment but also the heat treatment. The deep cooling treatment is to cool the coarse milled parts down to ~80K slowly in more than three hours and keep at 80K for two hours then slowly warmed up to room temperature in more than five hours. The heat treatment is to warm up the coarse milled parts slowly to 177 ℃ and then keep the temperature for eight hours. After that, they were cooled down naturally under non-circulating air condition to the room temperature. After the parts fabrication processes, we sent all the parts for Surtec 650 surface treatment to protect aluminum surfaces. The Surtec 650 is the replacement of the Alodine 1200S coating which is no longer available in Taiwan. We have tested the Surtec 650 coated sample with liquid nitrogen thermal cycles and no degradation was found in 10 rapid cycles. To reduce the scattered light, all parts will have black coating. For cartridge parts that locate close to the optical beam, they will be coated with Acktar black for the lowest reflectance. Other parts will be coated with Map AW Puk paint. We expect to start the integration tests in July 2024. Figure 15 shows some pictures of the FP2 components.

Figure 15. Picture of the FP2 wheel components. The left is the wheel body. The middle panel shows the spider vane and the right panel is a cartridge bed of a slit mask.

The dimensions of the manufactured parted were verified by CMM at 20 ℃. The slit dimensions were verified with microscopes. As the requirement of the slit width is critical, we measured the slit mask one by one and the dimension errors are around 3-5 μm which is well within the required accuracy.

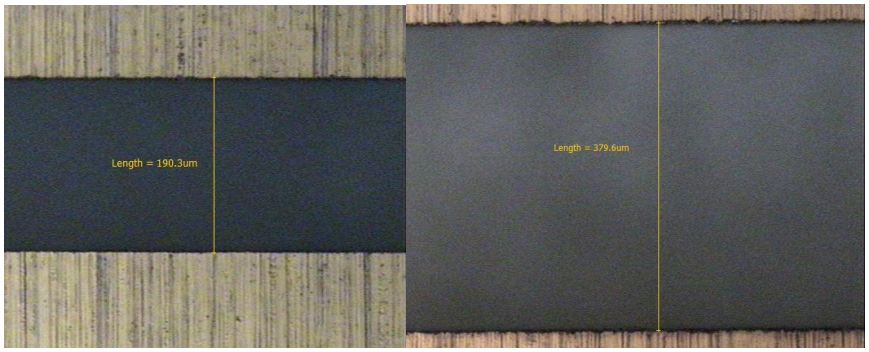

Figure 16. The microscope picture of the 189 μm (left) and 379 μm (right) slits.

5. SUMMARY

The design of the FP2 wheel assembly and the PP1 wheel assembly in the METIS CFO has been presented. The design has meet the various requirements especially the positioning accuracy and repeatability of the optical elements. The manufacturing of FP2 wheel is almost completed and we will soon start the manufacturing of the LMS pickoff wheel followed by the PP1 wheel assembly. We expect to deliver the FP2 wheel assembly in late 2024 and the PP1 wheel assembly in spring of 2025.

ACKNOWLEDGEMENTS

We gratefully acknowledge support from the Academia Sinica of Taiwan for the work carried out in ASIAA.

REFERENCES

[1] Brandl, B. et al., “METIS: The Mid-infrared ELT Imager and Spectrograph”, The Messenger, 182, 22-26, (2021)
[2] Bizenberger. P. et al., “METIS: final design of the imager sub-system”, Proc. SPIE 12184, 121843K, (2022)
[3] Bertram, T. et al., “METIS SCAO – implementing AO for ELT”, Adaptive Optics for Extremely Large Telescopes. Vol. 7. 23B, (2023)
[4] Rutowska, M. et al., “Warm calibration unit of the mid-infrared ELT instrument METIS: overview and current status towards FDR”, Proc. SPIE 12184, 121843M, (2022)
[5] METIS website, https://metis.strw.leidenuniv.nl/design-concept/

[6] Barriere. JC. et al., “Cryomechanism: A Cryogenic Rotating Actuator”, Proc. SPIE 8863, 886305, (2013)